Model-Free Adaptive Control of the Failing Heart Managed by Mechanical Supporting Devices

Jeongeun Son*, Yuncheng Du*

** Department of Chemical and Biomolecular Engineering, Clarkson University, Potsdam, NY 13676, USA (Tel: 315-268-2284; e-mail: ydu@clarkson.edu)*

Abstract: Left ventricular assist devices (LVADs)—mechanical circulatory pumps—have been used as a therapeutic option for patients who have progressed to the advanced stage of left-sided heart failure (HF), which is a chronic condition that the heart is unable to pump sufficient blood out of the left ventricle as it should. This surgically implanted device supports the native heart to pump blood from the heart to the remainder of the body to keep the patient alive as a temporary therapy until a donor's heart is available or as a destination therapy. However, the pump speed of the LVAD is typically set in a constant mode and cannot be freely changed. To promote the clinical use of LVADs as a long-term treatment option, a physiological control system is required to adaptively adjust the pump speed in response to time-varying blood demand. To this end, a model-free adaptive control (MFAC) algorithm is developed in this work, which estimates the control parameter over time using the data of manipulated and controlled variables (i.e., end-diastolic pressure of left ventricle and pump speed, respectively). In addition, since hemodynamic parameters in the cardiovascular system change over time due to short-term autonomic nerve regulation, we further considered baroreflex regulation to improve control performance; baroreflex regulation is one of the key factors of human's hemostatic mechanisms. The performance of the physiological controller is investigated and validated with computer simulations, which shows that the LVAD can respond to constant and time-varying blood demand.

Keywords: Left ventricular assist device, model-free adaptive control, time-varying physiological control, baroreflex regulation, cardiovascular system model.

1. INTRODUCTION

Heart failure (HF) is a critical condition that the heart cannot circulate enough blood to the body, which often requires heart transplants at the advanced stage. It is estimated that about 6.5 million adults in the U.S. have HF (Mensah, 2018), but not all patients can receive heart transplantation surgery due to mass donor shortages and health issues (e.g., impaired renal function or high pulmonary vascular resistance). As an alternative, left ventricular assist devices (LVADs) have been implanted in patients to provide temporary mechanical support for a failing left ventricle as a *bridge-to-transplant* until a donor's heart becomes available or a destination therapy for HF patients ineligible for heart transplants (Mancini and Colombo, 2015).

Cardiovascular models have become essential tools to study hemodynamics of the failing heart managed by an LVAD (Simaan et al., 2009; Son et al., 2020; Wang et al., 2015; Wu, 2004). Many numerical models describing the cardiovascular-LVAD system have been developed, which have different levels of complexity. For example, a lumped model of the cardiovascular system with LVAD support has been proposed (Simaan et al., 2009), which consists of six state variables. In this model, the right heart, including the right atrium and ventricle, and the pulmonary circulation, is assumed healthy and not studied. In addition, a more sophisticated model of the cardiovascular system has been developed to predict the hemodynamics of an LVAD recipient by including pulmonary circulation and venous circulation (Wang et al., 2015). In our previous work (Son et al., 2020), we developed a stochastic model of the cardiovascular-LVAD system to describe the systemic and pulmonary circulations, left atrium, left ventricle, right atrium, right ventricle, and an LVAD. This model can provide a probabilistic description of hemodynamics to improve accuracy. While these models are useful to investigate hemodynamics in the cardiovascular system managed by an LVAD, challenges remain to provide accurate predictions because the autonomic regulation of the cardiovascular system has not been considered in these models.

As a kind of short-term autonomic nerve regulation, baroreflex plays a key role in short-term pressure control. Specifically, it maintains the blood pressure stable by regulating neural effectors (Ottesen et al., 2004; Ursino, 1998). Due to such a baroreflex autoregulation mechanism, some parameters in the cardiovascular system can change over time, especially when the failing heart is managed by an LVAD (Liu et al., 2020). Thus, it is necessary to incorporate baroreflex response into the cardiovascular-LVAD model to provide accurate and autonomous predictions. It is worth mentioning that baroreflex regulation has been studied in several cardiovascular system models managed by LVADs (Bozkurt and Safak, 2013; Liu et al., 2020). However, the design of a feedback controller to automatically adjust the pump speed of an LVAD has not been studied, while taking into account the baroreflex regulation.

Currently, the pump speed of the LVAD is typically set at a constant speed by clinicians during the LVAD implantation surgery and cannot be freely adjusted afterward (Fetanat et al.,

2020; Meki et al., 2020; Wu, 2004). The main challenge for operating LVADs at constant speed is that undesirable cardiac events such as ventricular suction and regurgitation can happen, thus threatening health condition of HF patients. Specifically, the ventricular suction is a lethal event in which the pump attempts to withdraw more blood in the left ventricle than is available. When suction happens, it leads to ventricular collapse causing myocardial damage and right ventricular dysfunction. The regurgitation, backflow from the aorta to the left ventricle, can be induced when the pump speed is too low, which possibly develops recurrence of symptomatic heart failure and aortic valve failure (Meki et al., 2020; Wu, 2004). In addition, the blood demand changes with respect to different physiologic conditions (e.g., different physical activity levels). Thus, the design of a physiological control system is useful to mitigate these hazardous events and to provide sufficient blood perfusion for accounting for different blood need.

Different control methods for LVADs have been reported (Fu and Xu, 2000; Giridharan and Skliar, 2003; Simaan et al., 2009; Son et al., 2020), which can meet the time-varying blood need, while avoiding ventricular suction and regurgitation. For example, the constant differential pressure between the left ventricle and aorta was used to tune the pump speed over a wide range of physical activities in (Giridharan and Skliar, 2003); data of the predicted pump flow were used to adjust the pump speed in a control algorithm in (Simaan et al., 2009); and fuzzy logic-based controller was developed for the tunning of LVADs (Fu and Xu, 2000). However, most of the available control strategies only consider limited physiological changes to adjust the pump speed. In this case, the control performance cannot be guaranteed for a wide range of patients and heart conditions. To address this issue, a gain-scheduling control method was developed in (Son et al., 2020; Wang et al., 2015), but it requires an accurate cardiovascular-LVAD model for controller tuning, which is challenging to build and can be computationally impractical to adjust the pump speed in real-time, since the model is complicated and highly nonlinear.

To solve these challenges, in this work, we build a new model to combine the baroreflex regulation and the cardiovascular-LVAD model for accurate and reliable predictions. In addition, we develop a model-free adaptive control (MFAC) algorithm to adjust the control parameters for the tuning of the pump speed of LVADs over a wide range of physiological conditions. Specifically, the control strategy in this work can meet time-varying blood demand, while providing stable hemodynamics. It is worth mentioning that the MFAC-based control design was previously used to control LVADs (Fetanat et al., 2020), but the baroreflex was not considered, which can greatly affect the control performance and hemodynamics of the heart.

This paper is organized as follows. In Section 2, we present the cardiovascular system model that is managed by an LVAD and the baroreflex model that describes the autonomic nerve regulation, which can affect the short-term pressure control. Details about the feedback control design based on MFAC are given in Section 3, which are followed by the results of the computer simulation in Section 4. A brief conclusion is given in Section 5.

2. BACKGROUNDS

2.1 Cardiovascular-LVAD system model

Several models of the cardiovascular system managed by an LVAD have been developed, which have various complexity levels. In this study, the cardiovascular model is built based on existing works (Fernandez de Canete et al., 2013; Simaan et al., 2009; Wu, 2004) to consider both sides of the failing heart, the feedback controller of LVADs, and the baroreflex regulation. This model has thirteen state variables, describing the systemic and pulmonary circulations, left atrium and ventricle (LA and LV), right atrium and ventricle (RA and RV), and an LVAD, as in (Son et al., 2020):

$$\frac{d\boldsymbol{x}}{dt} = \boldsymbol{A}(t)\boldsymbol{x} + \boldsymbol{B}(t)p(\boldsymbol{x}) + cv(t) \tag{1}$$

where $\boldsymbol{x}$ is a vector of states variables of the cardiovascular-LVAD model (i.e., x_1 to x_{13} listed in Table 1), $\boldsymbol{A}(t)$ and $\boldsymbol{B}(t)$ represent 13×13 and 13×4 time-varying matrices. In addition, $p(\boldsymbol{x})$ is a vector to mimic the nonlinear behavior of heart valves, and c is a 13×1 constant vector. Lastly, $v(t)$ is the control variable of the LVAD represented with $v(t) = \omega^2$, where ω is the pump speed. Details of the model in (1) and its parameters can be found in (Son et al., 2020).

Table 1. State variables in the cardiovascular-LVAD model (Son et al., 2020)

Variable		Description	Unit
$x_1(t)$	$AoP(t)$	Aortic pressure	*mmHg*
$x_2(t)$	$Q_{AS}(t)$	Arterial systemic circulation blood flow	*ml/s*
$x_3(t)$	$ASP(t)$	Arterial systemic pressure	*mmHg*
$x_4(t)$	$Q_{VS}(t)$	Venous systemic circulation blood flow	*ml/s*
$x_5(t)$	$RAP(t)$	Right venous-atrial pressure	*mmHg*
$x_6(t)$	$RVP(t)$	Right ventricular pressure	*mmHg*
$x_7(t)$	$PAP(t)$	Pulmonary artery pressure	*mmHg*
$x_8(t)$	$Q_{AP}(t)$	Arterial pulmonary circulation blood flow	*ml/s*
$x_9(t)$	$APP(t)$	Arterial pulmonary pressure	*mmHg*
$x_{10}(t)$	$Q_{VP}(t)$	Venous pulmonary circulation blood flow	*ml/s*
$x_{11}(t)$	$LAP(t)$	Left venous-atrial pressure	*mmHg*
$x_{12}(t)$	$LVP(t)$	Left ventricular pressure	*mmHg*
$x_{13}(t)$	$Q_P(t)$	LVAD Pump flow	*ml/s*

In this model, there are four hemodynamic parameters that can be used to define different physiological states, which includes the systemic vascular resistance (SVR or R_s), the pulmonary vascular resistance (PVR or R_{pv}), maximum elastance of the left ventricle ($E_{max,lv}$), and the heart rate (HR). Among them, the resistance R_s is the most representative parameter to define the physical activity level. For example, when HF patients are active (e.g., mild exercise), a smaller value of R_s is used. The elastance function, which is defined as the inverse of each ventricular compliance, i.e., $E(t) = 1/C(t)$, can be given as in (Stergiopulos et al., 1996):

$$E(t) = (E_{max} - E_{min})\bar{E}(\bar{t}) + E_{min} \tag{2}$$

where $\bar{E}(\bar{t})$ is the normalized elastance function, also referred to as "double hill" function (Stergiopulos et al., 1996), $\bar{t}$ is the normalized time defined as $\bar{t} = t/(0.2 + 0.15T)$ and T is the heart period (Simaan et al., 2009). In addition, E_{max} and E_{min} are the maximum and the minimum elastance of each

ventricle, respectively. The maximum elastance E_{max} can be used as an indicator to represent the severity levels of HF.

To describe the pump dynamics of LVADs, a semiempirical model is used in this work (Choi et al., 1997), which is based on the correlation among the pressure difference H across the pump, pump speed, and pump flow as in:

$$H = \gamma_0 x_{13} + \gamma_1 \frac{dx_{13}}{dt} + \gamma_2 v^2 \quad (3)$$

where γ_0, γ_1, and γ_2 are pump-dependent coefficients, each value of which can be found in the literature (Simaan et al., 2009).

2.2 Baroreflex Regulation

Baroreflex response contributes to short-term pressure control to maintain the blood pressure stable (Liu et al., 2020; Ottesen et al., 2004). Accordingly, it causes some of the hemodynamic parameters in the model to change over time. To incorporate the baroreflex regulation with the cardiovascular-LVAD model presented in Section 2.1, the baroreflex model, which was proposed in (Ursino, 1998) and slightly modified in (Liu et al., 2020), is adopted in this work. This model consists of the afferent pathway, efferent neural pathways, and effectors, which are discussed below.

The afferent neural pathway carries signals sensed by the baroreceptors to the central nervous system (i.e., the brain). In this model, the afferent neural pathway is described by two properties such as the relationship between afferent nerve activity and arterial pressure and the sensitivity of arterial baroreceptors to the arterial pressure and its rate of change. The efferent neural pathways are modeled by the relation between the frequency of spikes in the sinus nerve and the frequency of the sympathetic fibers and vagal activity. These stimulation activities, i.e., stimulation of sympathetic nerves, result in dynamic changes of the effectors in the cardiovascular model (Ursino, 1998). As reported in (Liu et al., 2020), the baroreflex model in this work controls four effectors, such as systemic vascular resistance (SVR or R_s), maximum elastance of the left and right ventricles ($E_{max,lv}$ and $E_{max,rv}$), and heart period (T). Each effector controlled by baroreflex regulation can be mathematically represented as in:

$$\delta(t) = \delta_0 + \Delta\delta(t) \quad (4)$$

where the generic parameter δ is used to represent each effector over time; δ_0 is each parameter in the absence of vagal and sympathetic activities; $\Delta\delta$ is the parameter change caused by sympathetic stimulation. Details on the description of the baroreflex model are given in (Liu et al., 2020; Ursino, 1998).

In this work, we combined the baroreflex response with the cardiovascular-LVAD model, resulting in a detailed model of the heart defined by nineteen state variables. For clarity, Fig. 1 illustrates the cardiovascular-LVAD model coupled with the baroreflex model. As seen, the model presented in Section 2.1 can be executed to simulate the arterial pressure (i.e., x_1 in Table 1). Then, the baroreflex model senses this information and sends a signal toward the central nervous system through afferent pathways. From the central nervous system, the efferent pathways carry this signal away by regulating a few distinct neural effectors. Consequently, the updated effectors alter hemodynamic in the cardiovascular-LVAD system.

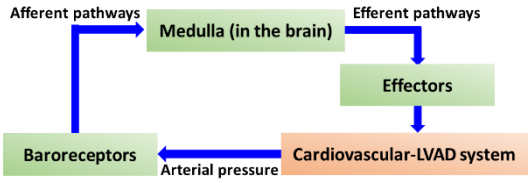

Figure 1. Illustration of the cardiovascular-LVAD system coupled to the baroreflex model.

2.3 Model-Free Adaptive Control

In this work, model-free adaptive control (MFAC) is employed to design a physiological control system, which is a type of data-driven control method. Most adaptive control methods in the literature are tuned to achieve desired control performance for patients under certain heart conditions. In this case, the control performance cannot be guaranteed across the wider inter- and intra-patient variations in the cardiovascular-LVAD system. However, the MFAC algorithm used in this work can adjust its controller gain over time, thereby allowing us to deal with changes in process dynamics and disturbances, which can be beneficial for controlling the LVAD pump under the time-varying nature of the cardiovascular system (Fetanat et al., 2020). Specifically, the data-driven MFAC is implemented by establishing a dynamic linearization data model between the input and output of the controlled system, then estimating the control parameter named pseudo-partial derivative (PPD) at each operation point online (Hou and Jin, 2013). A brief description of MFAC is given as follows.

For simplicity, let consider a nonlinear discrete-time system of single-input, single-output (SISO), which can be defined as in:

$$y(k+1) = f\big(y(k), \dots, y\big(k - n_y\big), u(k), \dots, u(k - n_u)\big) \quad (5)$$

where $y(k)$ represents the system output (i.e., the controlled variable—end-diastolic pressure of left ventricle); $u(k)$ is the input (i.e., manipulated variable—pump speed) at time instant k; and f is an unknown nonlinear function. In addition, the integers n_y and n_u are unknown orders of the system output and the control input, respectively. This nonlinear system can be defined by the dynamic linearization data model as in:

$$y(k+1) = y(k) + \emptyset(k)\Delta u(k) \quad (6)$$

where the time-varying parameter $\emptyset(k)$ is called PPD. This parameter is unknown and needs to be estimated at each time instant k such that the SISO system described in (5) is represented with the model (6). By minimizing the differences between the desired and system outputs (i.e., $y^*(k+1) - y(k)$) and two consecutive control inputs (i.e., $\Delta u(k)$), the control input can be derived as in (Hou and Jin, 2013):

$$u(k) = u(k-1) + \frac{\rho\emptyset(k)\big(y^*(k+1) - y(k)\big)}{\lambda + \|\emptyset(k)\|^2} \quad (7)$$

where y^* is the desired reference of system output y, ρ is a step factor added to make (7) more general, and λ indicates a

weighting constant to restrict the changing rate of the control input u. It is important to note that the time-varying parameter $\emptyset(k)$ is unknown and has to be estimated. By using the PPD estimation algorithm in (Hou and Jin, 2013), the unknown parameter PPD can be found as below:

$$\widehat{\emptyset}(k) = \widehat{\emptyset}(k-1) + \frac{\eta \Delta u(k-1)\left(\Delta y(k) - \widehat{\emptyset}(k-1)\Delta u(k-1)\right)}{\mu + \|\Delta u(k-1)\|^2} \quad (8)$$

$$\widehat{\emptyset}(k) = \widehat{\emptyset}(1), if\ \left|\widehat{\emptyset}(k)\right| \le \varepsilon\ or\ |\Delta u(k-1)| \le \varepsilon\ or\ sign(\widehat{\emptyset}(k)) \ne sign(\widehat{\emptyset}(1))$$

where $\widehat{\emptyset}(k)$ denotes the estimated PPD, and $\widehat{\emptyset}(1)$ is the initial value of $\widehat{\emptyset}(k)$. In addition, μ is a weighting constant, η is a step factor added to make (8) more general and flexible, and ε is a small positive constant. Similar to (7), the PPD estimation in (8) is obtained by minimizing the squared error of the model (i.e., $\Delta y(k) - \widehat{\emptyset}(k-1)\Delta u(k-1)$ in (6)) and changes in two consecutive PPD parameters (i.e., $\Delta\widehat{\emptyset}(k)$). Details on the derivation of these expressions and their assumptions can be found in (Hou and Jin, 2013).

3. METHODOLOGY

As noted in Section 2.1, the most representative parameter to define the physical activity level in the cardiovascular-LVAD model is systemic vascular resistance (SVR or R_s). Thus, in this work, we only focus on changes in R_s to investigate the control performance. The control objective in this work is to automatically adjust the pump speed with respect to different levels of physical activity, while providing sufficient perfusion and avoiding suction.

In this work, the manipulated variable is the pump speed of an LVAD, and left ventricular end-diastolic pressure (LVEDP)—the left ventricular pressure at the end of diastole of the heart—is chosen as the controlled variable, since it is recognized as an efficient parameter to mimic the native heart's hemodynamics in other physiological control strategies (Fetanat et al., 2020; Pauls et al., 2016). Also, LVEDP is an important measure of ventricular performance to indicate clinical symptoms of HF patients (e.g., pulmonary hypertension or right-sided heart failure) as in (Landsberg, 2018). For clarity, Fig. 2 shows the general block diagram of the feedback control strategy used in this study.

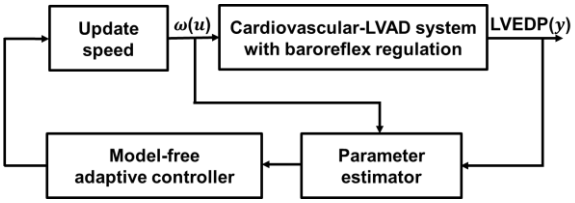

Figure 2. Schematic of the model-free adaptive controller for the cardiovascular-LVAD system

As seen in Fig. 2, once the measurements of the controlled variable (LVEDP or y) and the manipulated variable (pump speed ω or u) are available, the PPD parameter $\widehat{\emptyset}$ in MFAC is estimated by (8). Then, the estimated $\widehat{\emptyset}$ is used to update the pump speed by the update rule of MFAC as in (7). Lastly, the updated pump speed controls the LVAD in the cardiovascular system under baroreflex regulation, providing a new value of the controlled variable at each loop.

To show the control performance for the constant and time-varying physical activity level of an LVAD recipient, two case scenarios are investigated in this work. For each scenario, we designed the MFAC control system to maintain the controlled variable LVEDP at a constant value, which will be described in Section 4 with simulations.

4. RESULTS

4.1 Cardiovascular-LVAD model under baroreflex response

To test and validate the model in this work that combines the cardiovascular-LVAD model in Section 2.1 with the baroreflex response in Section 2.2, several hemodynamic variables are simulated, which include left ventricular pressure (LVP, x_{12}), aortic pressure (AoP, x_1), arterial flow (Q_{AS}, x_2) and pump flow(Q_P, x_{13}). The simulation results of consecutive cardiac cycles from 58 to 60 seconds are given in Fig. 3.

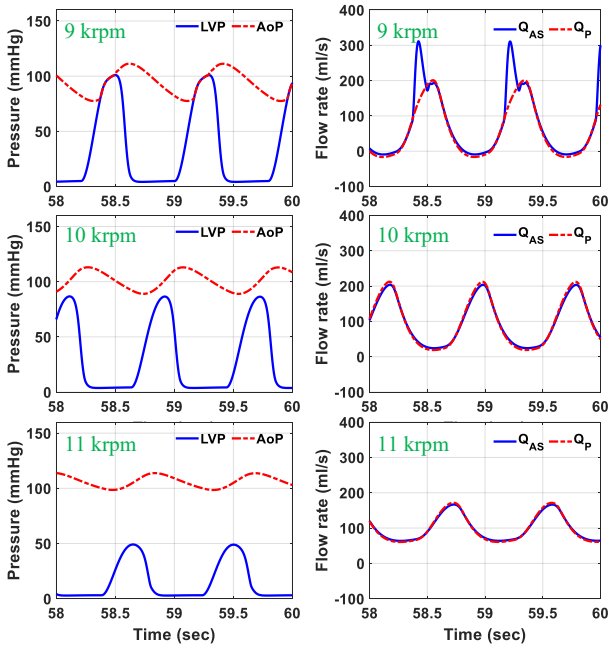

Figure 3. Simulation results of the hemodynamic variables in the presence of baroreflex regulation with different pump speeds of an LVAD. (Left ventricular pressure (LVP) and aortic pressure (AoP); arterial flow (Q_{AS}) and the pump flow (Q_P))

As seen in Fig. 3, with the increase of pump speed, it was found that the left ventricular pressure decreases; the aortic pressure slightly increases; the pulsatility of the pump flow decreases, showing stable and periodic predictions. In addition, as can be seen, the heart period, the length of time corresponding to one cardiac cycle, is different depending on the pump speed due to the baroreflex regulation involved in the model. Specifically, the heart period in the third row of Fig. 3 is longer than the results in the first two rows. Note that the generic parameter

values in the absence of vagal and sympathetic activities, i.e., δ_0 in (4), i.e., $R_{s,0}$, T_0, $E_{max,lv0}$, and $E_{max,rv0}$, are set to 0.71 mmHg·s/mL, 0.52 sec, 1.0 mmHg/ml and 0.6 mmHg/ml, respectively (Liu et al., 2020). Combining the cardiovascular model with the baroreflex regulation, each generic parameter δ in (4) keeps changing and eventually reaches a stable value. The resulting parameters of the effectors R_s, T, $E_{max,lv}$, and $E_{max,rv}$ at the given pump speed are summarized in Table 2. It was found that as the pump speed increases, three parameters, i.e., R_s, $E_{max,lv}$, and $E_{max,rv}$, decreases, while the heart period T increases. This observation is consistent with the results in (Liu et al., 2020), which clearly shows the accuracy of the cardiovascular-LVAD model in this work, which can consider the baroreflex regulation and the effect of LVAD on the heart.

Table 2. Simulated effectors controlled by the baroreflex regulation for three different pump speeds of the LVAD

Pump speed	R_s	T	$E_{max,lv}$	$E_{max,rv}$
9 krpm	1.0450	0.7930	1.1712	0.8796
10 krpm	1.0069	0.8064	1.1524	0.8490
11 krpm	0.9240	0.8523	1.1122	0.7832

4.2 Control performance of the model-free adaptive control

4.2.1 Constant systemic vascular resistance.

In the first case scenario, we assume that the patient's activity level remains unchanged for a long time. Thus, a constant value of R_s is considered to describe the unchanged physical activity of an LVAD recipient. Since the parameter R_s can change over time due to the baroreflex regulation involved in the model, we fix the parameter δ_0 for R_s (i.e., $R_{s,0}$) in (4) to 0.71 mmHg·s/mL in this work. Note that the MFAC used in this work adjusts the pump speed of LVADs to minimize the error between the controlled variable and the set point, and the MFAC parameters, i.e., ρ, λ, η, and μ in (7) and (8), were set to 1, 0.45, 2, and 0.5, respectively, which were chosen empirically. Fig. 4 shows the simulation results of the pump speed and the corresponding pump flow, the PPD estimation, and the control error between the set point and the dynamic values of the controlled variable (LVEDP). Due to the space limit, only the noise-free simulations are shown in this study.

As can be seen from Fig. 4, the pump speed keeps increasing to meet the physiological demand and reaches a steady-state with sufficient setting time, without inducing a suction. It is worth noting that the onset of suction can be characterized by two signatures, which are (i) a significant change in the minimum pump flow in consecutive cardiac cycles and (ii) a large variation in the flow signal after the onset of suction. Clearly, the pump flow as in Fig. 4 (b) does not have any of these signatures to indicate the onset of suction. Detailed descriptions for identifying the onset of suction can be found in (Ferreira et al., 2009; Simaan et al., 2009; Son et al., 2020). In addition, as shown in Fig. 4 (c), the PPD parameter $\widehat{\emptyset}$ of the MFAC is time-varying and estimated over time by (8). Accordingly, the error between the set point and the controlled variable (i.e., LVEDP) eventually converges to zero. Note that the MFAC exhibits time-invariant PPD parameter after around 80 secs. This is because the change in two consecutive parameters $\widehat{\emptyset}$ is smaller than the predefined small constant ε as defined in (8). This clearly shows that the MFAC here can adaptively adjust the control parameter using the input/output data of the cardiovascular-LVAD system.

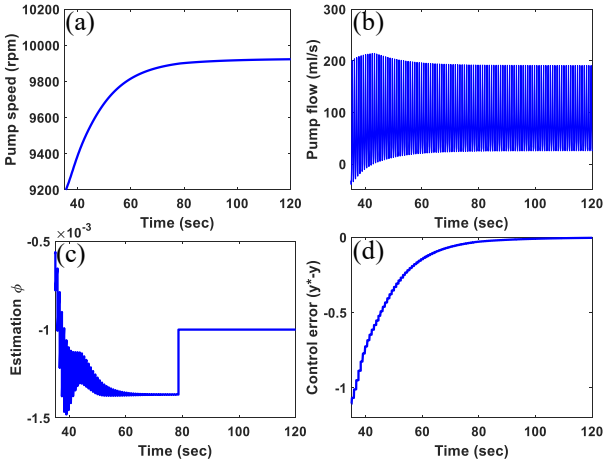

Figure 4. Simulation results of the MFAC for a constant level of physical activity, while considering the baroreflex regulation. (a) pump speed, (b) pump flow, (c) PPD estimation, and (d) control error.

4.2.2 Time-varying systemic vascular resistance.

In the second case study, it is assumed that the parameter $R_{s,0}$ in (4) changes over time, which can be used to define changes in the physical activity level of a HF patient. For the first 150 sec, $R_{s,0}$ was set to 0.71 mmHg·s/mL by assuming that the status of the patient was resting. For the rest of the simulation time, $R_{s,0}$ was set to 0.21 mmHg·s/mL to represent the mild exercise of the patient, e.g., walking stairs. The result of the MFAC-based control design is shown in Fig. 5.

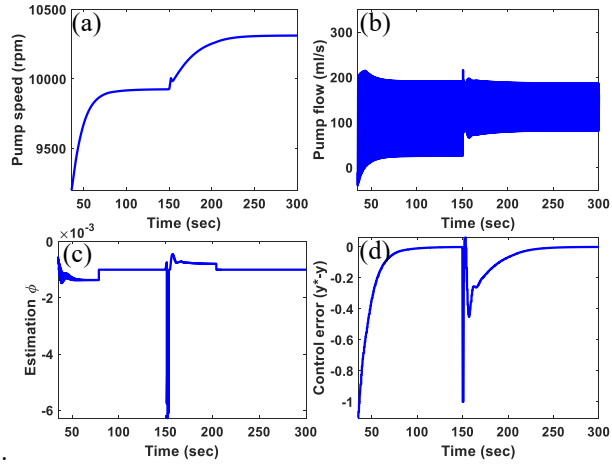

Figure 5. Simulation results of the MFAC for time-varying level of physical activity, while considering the baroreflex regulation. (a) pump speed, (b) pump flow, (c) PPD estimation, and (d) control error.

As seen in Fig. 5 (a), the controller can appropriately adjust the pump speed with respect to the changes in the physical activity level to meet blood perfusion demand. Specifically, the pump speed of the LVAD can converge to a specific speed for each

value of $R_{s,0}$, i.e., each level of physical activity. Note that the settling time in Fig. 5 (a) can be changed by the MFAC control parameters. In addition, as observed in the results of the constant $R_{s,0}$, any signature to indicate an onset of suction is not found in the resulting pump flow during the adjustment of the pump speed as shown in Fig. 5 (b). Furthermore, Fig. 5 (c) and (d) show the simulation results of the time-varying PPD parameter $\widehat{\emptyset}$ in MFAC and the error between the set point (i.e., LVEDP) and the values of the controlled variable. When the patient's activity level is changed at around 150 sec, a sharp change is observed in each result. This shows that the MFAC-based controller can quickly respond to a new hemodynamic in the cardiovascular system under the baroreflex regulation that may result from a change in the physical activity level.

5. CONCLUSIONS

In this current work, we develop a model that combines the cardiovascular-LVAD model with the baroreflex regulation to consider the effect of the short-term autonomic regulation on the control design of an LVAD. To automatically adjust the pump speed of an LVAD, a model-free adaptive control, one of the data-driven control methods, was employed, where left ventricular end-diastolic pressure was used as the feedback variable. To validate the performance of the controller, two different case scenarios were investigated, representing constant level and time-varying levels of physical activity of a HF patient. The simulation results show that the controller can adapt to a new physiological state caused by a change in the level of physical activity and can adaptively adjust the control parameter over time with the input/output data only. Future work will involve validating the performance of the algorithm through comparison with previously developed algorithms for LVAD including standard PID control.

REFERENCES

Bozkurt, S., and Safak, K.K. (2013). Evaluating the hemodynamical response of a cardiovascular system under support of a continuous flow left ventricular assist device via numerical modeling and simulations. *Computational and Mathematical Methods in Medicine*, 2013, 986430.

Choi, S., Boston, J.R., Thomas, D., and Antaki, J.F. (1997). Modeling and identification of an axial flow blood pump. In *Proceedings of the 1997 American Control Conference*, volume 6, 3714–3715. IEEE.

Fernandez de Canete, J., Del Saz-Orozco, P., Moreno-Boza, D., and Duran-Venegas, E. (2013). Object-oriented modeling and simulation of the closed loop cardiovascular system by using SIMSCAPE. *Computers in Biology and Medicine*, 43(4), 323–333.

Ferreira, A., Boston, J.R., and Antaki, J.F. (2009). A control system for rotary blood pumps based on suction detection. *IEEE Transactions on Biomedical Engineering*, 56(3), 656–665.

Fetanat, M., Stevens, M., Hayward, C., and Lovell, N.H. (2020). A physiological control system for an implantable heart pump that accommodates for interpatient and intrapatient variations. *IEEE Transactions on Biomedical Engineering*, 67(4), 1167–1175.

Fu, M., and Xu, L. (2000). Computer simulation of sensorless fuzzy control of a rotary blood pump to assure normal physiology. *ASAIO Journal*, 46(3), 273–278.

Giridharan, G.A., and Skliar, M. (2003). Control strategy for maintaining physiological perfusion with rotary blood pumps. *Artificial Organs*, 27(7), 639–648.

Hou, Z., and Jin, S. (2013). *Model Free Adaptive Control: Theory and Applications*. CRC Press.

Landsberg, J.W. (2018). *Manual for Pulmonary and Critical Care Medicine*. Elsevier.

Liu, H., Liu, S., Ma, X., and Zhang, Y. (2020). A numerical model applied to the simulation of cardiovascular hemodynamics and operating condition of continuous-flow left ventricular assist device. *Mathematical Biosciences and Engineering*, 17(6), 7519–7543.

Mancini, D., and Colombo, P.C. (2015). Left ventricular assist devices: a rapidly evolving alternative to transplant. *Journal of the American College of Cardiology*, 65(23), 2542–2555.

Meki, M., Wang, Y., Sethu, P., Ghazal, M., El-Baz, A., and Giridharan, G.. (2020). A sensorless rotational speed-based control system for continuous flow left ventricular assist devices. *IEEE Transactions on Biomedical Engineering*, 67(4), 1050–1060.

Mensah, G.A. (2018). Heart failure in low-income and middle-income countries: rising burden, diverse etiology, and high mortality. *Journal of Cardiac Failure*, 24(12), 833–834.

Ottesen, J.T., Olufsen, M.S., and Larsen, J.K. (2004). *Applied Mathematical Models in Human Physiology*. Society for Industrial and Applied Mathematics.

Pauls, J.P., Stevens, M.C., Bartnikowski, N., Fraser, J.F., Gregory, S.D., and Tansley, G. (2016). Evaluation of physiological control systems for rotary left ventricular assist devices: an in-vitro study. *Annals of Biomedical Engineering*, 44(8), 2377–2387.

Simaan, M.A., Ferreira, A., Chen, S., Antaki, J.F., and Galati, D.G. (2009). A dynamical state space representation and performance analysis of a feedback-controlled rotary left ventricular assist device. *IEEE Transactions on Control Systems Technology*, 17(1), 15–28.

Son, J., Du, D., and Du, Y. (2020). Modelling and control of a failing heart managed by a left ventricular assist device. *Biocybernetics and Biomedical Engineering*, 40(1), 559–573.

Stergiopulos, N., Meister, J.J., and Westerhof, N. (1996). Determinants of stroke volume and systolic and diastolic aortic pressure. *American Journal of Physiology-Heart and Circulatory Physiology*, 270(6), H2050–H2059.

Ursino, M. (1998). Interaction between carotid baroregulation and the pulsating heart: a mathematical model. *American Journal of Physiology-Heart and Circulatory Physiology*, 275(5), H1733–H1747.

Wang, Y., Koenig, S.C., Slaughter, M.S., and Giridharan, G.A. (2015). Rotary blood pump control strategy for preventing left ventricular suction. *ASAIO Journal*, 61(1), 21–30.

Wu, Y. (2004). *Design and testing of a physiologic control system for an artificial heart pump* [Ph.D. dissertation, University of Virginia].